Analyzing environmental factors that favor the growth of the invasive brown macroalga *Rugulopteryx okamurae* (Ochrophyta): The probable role of the nutrient excess

Jesús M. Mercado[1], Francisco Gómez-Jakobsen[1], Nathalie Korbee[2], Antonio Aviles[2], José Bonomi-Barufi[3], María Muñoz[4], Andreas Reul[2], Félix L. Figueroa[2]

[1]Centro Oceanográfico de Málaga, Instituto Español de Oceanografía-CSIC, Puerto Pesquero s/n. 29640, Fuengirola, Málaga. Spain

[2]Universidad de Málaga, Instituto de Biotecnología y Desarrollo Azul (IBYDA). Departamento de Ecología y Geología. Facultad de Ciencias. Campus Universitario de Teatinos s/n 29071 Málaga, Spain

[3]Phycology Laboratory, Botany Department, Federal University of Santa Catarina, 88049-900, Florianopolis, SC, Brazil

[4]Centro Oceanográfico de Baleares, Instituto Español de Oceanografía-CSIC, Muelle de Poniente s/n, 07015, Palma de Mallorca, Spain

*Corresponding author: jesus.mercado@ieo.es

ABSTRACT

Time series of temperature, salinity and nutrients in the Strait of Gibraltar (SoG) were researched to analyze which factors explain the invasive success of *Rugulopteryx okamurare*, which has colonized wide coastal areas at the Spanish and Moroccan coasts since 2016. Temperature and salinity were higher in the SoG compared to its native habitat, implying that the alga is active during the whole seasonal cycle and grows optimally at the high salinities occurring in the SoG. Nitrate removal experiments indicate that the alga is able to linearly increase its N uptake rates following boost in nitrate concentration. Furthermore, *R. okamurae* N content ranged from 1.4% to 4.5% suggesting that this species has high N storage capacity potentially usable when the external N concentration decreases. These physiological characteristics would explain sharp growth of the alga in the SoG where high N concentrations are registered occasionally.

Key words: inorganic nutrients, invasive species, nitrate uptake, *Rugulopteryx okamurae*, salinity, temperature.

1. Introduction

Regional studies have identified hundreds of non-indigenous marine species introduced by humans, including tens of macroalgae (Ribera Siguan, 2002; Zenetos and Galanili, 2020). At least 30% of non-indigenous macroalgae have produced impacts on the native ecosystems worldwide (Davidson et al., 2015) such as monopolization of the space and drastic reduction of the abundance and diversity of the native species, which are indicative of invasive behavior. Little attention has been paid to the reasons why some macroalgal species which do not feature an invasive behavior in their natural distribution areas, are able to colonize opportunistically other areas once entered. Overall, ecosystem imbalances produced by natural and/or anthropogenic changes would explain the success of introduced species (Shaffelke et al., 2006). Notorious examples of seaweed invasions or extreme algal blooms favored by human perturbations are those ones produced by *Undaria pinnatifida* in coastal areas of Europe and Argentina (Meretta et al., 2012; Kraan, 2016), *Ulva prolifera* in the Yellow sea and East China Sea (Zhao et al., 2019), *Sargassum* sp. in the Caribbean sea (Franks et al., 2016; Wang et al., 2019; Chávez et al., 2020) and *Caulerpa taxifolia* in the Mediterranean Sea (Meinesz et al., 1993, 2001).

It is widely accepted that the climate change combined with other anthropogenic impacts (e.g. eutrophication and acidification) play a major role in determining the colonizing success of non-native species (Diez et al., 2012). In fact, anthropogenic disturbances have been identified as the further determining factor for some seaweeds invasions (Davidson et al., 2015). For instance, physical alterations of habitat produced by storms (Scheibling and Gagnon, 2006) and/or great amount of nutrient discharges associated to pollution gave competitive advantage to some opportunistic non-native species in different ecosystems (Piazzi et al. 2001, 2005, 2016;

Boudouresque and Berlaque, 2002; Piazzi and Balata 2009; Lapointe and Bedford, 2011; Gennaro and Piazzi, 2014). Biotic factors such as release of natural herbivorous with feeding preference on the native communities might also contribute to the success of the invasive macroalgae (Vermeij et al., 2009, Noè et al., 2018).

The Mediterranean Sea is the region with the highest number of introduced macroalgal species with more than hundred non-indigenous species documented so far (Boudouresque and Verlaque, 2005; Williams and Smith, 2007). Approximately a dozen of these species have shown invasive traits (Verlaque and Fritayre, 1994; Piazzi and Cinelli, 2003). The brown macroalga *Rugulopteryx okamurae* (Dawson) I.K.Hwang, W.J. Lee & H.S.Kim (Dictyotales, Ochrophyta) has been recently added to this list of invasive species due to it is invading the coasts of the Alboran Sea in the Western Mediterranean Sea from 2016 (García-Gómez et al., 2017, 2020; El Aamri et al., 2018). Recently it is starting to invade areas in Provence coast in France (Ruitton et al., 2021) and the Portugal coast (Faria et al., 2021). This algal species originated from East Asia (China, Japan, Korea; DeClerck et al., 2006) was identified by the first time in the Mediterranean Sea by 2002 in the Thau Lagoon, where its entering was associated to oyster aquaculture (Verlaque et al., 2009). The alga grew in the lagoon from that date (Boudouresque et al., 2011) without showing an invasive trait. In contrast, from its first detection in 2015, *R. okamurae* has colonized wide areas of the rocky shore in the southern and northern coasts of the Strait of Gibraltar (SoG). Large biomass accumulations were recorded for the first time in July 2016 (Altamirano-Jeschke et al., 2016) reaching its maximum growth in 2017 when almost 100% of coastal habitats from surface to 15 m depth at the SoG north part (within the marine protected area *Natural Park of The Estrecho*) were occupied. Consequently, only two years from its first detection, drastic alterations in the biodiversity of the native communities

coinciding with sharp growth of *R. okamurae* have been produced (García-Gómez et al., 2021). Nowadays, its impact continues to be severe since thalli of this species are frequently washed ashore in the north of the Alboran Sea, forcing their cleaning and impacting significantly on the tourism activity. The nets of fishing vessels in the SoG are often collapsed by *R. okamurae* floating thalli even in areas far from the shore, producing significant economic loss.

Despite the impacts produced by *R. okamurae*, the factors that triggered this invasion in the SoG still remain little known. Most studies published so far mention simplistically the temperature as a possible cause favoring the invasion. However, the oceanic circulation at the SoG produces conspicuous interannual, seasonal and short-term variability in temperature, salinity and nutrients (García-LaFuente et al., 2000; Gómez et al., 2004; Gómez-Jakobsen et al., 2019); additionally, the area receives significant inputs of inorganic nutrients from land sources (Mercado et al., 2018). Therefore, it is tricky to attribute the invasion of *R. okamurae* to a particular environmental factor without an exhaustive analysis of its variability patterns. In this work, we analyzed time series of temperature, salinity and inorganic nutrients covering a wide time period that includes the first phases of the invasion. The environmental conditions in the study area were compared with the origin habitat of *R. okmurae* and its possible competitive advantages were researched. Particularly, we investigated if the alga capacity for assimilating dissolved inorganic nitrogen could be relevant in determining its success in the SoG. Based on these analyses, we hypothesized that changes in the hydrological circulation patterns combined with nutrient pollution might be an important factor that favored the growth of *R. okamurae* at the study area.

2. Material and Methods

2.1. Gathering of meteorological and oceanography data

Time series of air and water temperature and satellite chlorophyll *a* were built with daily data gathered for the period 2010-2019. The daily data of air temperature were obtained from a meteorological station located in the town of Tarifa (Spanish Meteorological Agency, http://www.aemet.es; Fig. 1). Daily means of temperature provided by a temperature sensor moored in the coast at 33 m depth (36.00ºN, 5.59ºW; Puertos del Estado) were also collected for the same period. Ocean color data for a location nearby the Strait of Gibraltar were retrieved from the platform MODIS-Aqua (reflectances at 443, 488 and 547 nm were used). This satellite provides a daily image of the study zone with a spatial resolution of 1.1 km^2. Level 2 scenes (reprocessing 2018) from August 2002 to October 2019 were downloaded from the NASA-Ocean Color website (https://oceancolor.gsfc.nasa.gov/). Those scenes inadequate for the analysis due to sun glitter and/or the presence of clouds or fog were discarded, and only valid scenes were used. Satellite chlorophyll *a* concentrations were calculated from the reflectance values by using the algorithm SMED3M (Gómez-Jakobsen et al., 2018). The daily data were weekly averaged prior to be analyzed statistically.

Outputs of a 3D high-resolution biogeochemical multi-year model for the SoG (36.00ºN, 5.58ºW; Fig. 1) were downloaded from the E.U. Copernicus Marine Service (https://resources.marine.copernicus.eu; product: IBI_MULTIYEAR_BGC_005_003; processing level: L4). IBI-MFC product is based in an application of the biogeochemical model PISCES running simultaneously with the ocean physical IBI reanalysis, generating both products at the same horizontal resolution of 1/12°. The retrieved modeled variables at 1 m depth included salinity, nitrate, phosphate, mixed

layer depth (MLD), transparency and meridional (S-N) and zonal (W-E) components of the current velocity. Monthly time series of each variable were used to analyze trends.

In order to research the nutrient conditions in the invaded area, concentrations of nitrate, nitrite, ammonium and phosphate obtained in coastal stations located nearby or within the invaded area were downloaded from a database of the Andalusian Regional Government (*Visor de la Calidad de las Aguas de Andalucía* https://laboratoriorediam.cica.es/Visor_DMA; Consejería de Agricultura, Ganadería, Pesca y Desarrollo Sostenible de la Junta de Andalucía; Fig. 1). These stations are sampled several times each year within monitoring programs for implementation of the EU Water Framework Directive. Additionally, nutrient concentrations in the water column at a station located in the outer part of the Algeciras Bay (36.02ºN, -5.38ºW; Fig. 1) were used to characterize the nutrient composition of the seawater that flows in the study area. These offshore station data were obtained during different research surveys performed quarterly in 2011-2012, 2014-2015 and 2019 by the Spanish Institute of Oceanography-CSIC. In these cruises, water samples were obtained at different depths with Niskin bottles and the nutrients were analyzed in the laboratory following the protocols published in Ramírez et al. (2005) by means of segmented flow analyzer QuAAtro 39 (Seal Analytical).

2.2. Measurements of the physiological performance

Experiments of nitrate removal were conducted with algae collected at the Caleta beach (Tarifa) on 16th October 2019. Thalli attached to rocks were selected and rapidly transported in icebox to the laboratory where were washed with seawater and epiphytes were removed. About 2 g of cleaned thalli were placed into 1 L methacrylate flasks containing 38.0 salinity seawater enriched with 50 μM of $NaNO_3$ as N source at 22 ºC.

The culture was vigorously aerated and illuminated with 200 μmol photons m^{-2} s^{-1} of irradiance emitted from white light LEDs (RGB) at photoperiod of 12h:12h (light:dark). Thalli acclimated to these conditions for one week were used to determine the nitrate uptake kinetics. Different initial concentrations of nitrate were tested by adding small amounts of a solution of $NaNO_3$ to the culture flasks containing fresh weight (FW) 2 g of acclimated thalli. The nominal initial concentrations of nitrate were: 50, 100, 160, 250, 400 and 800 μM. Each concentration was tested by triplicate for 7 days. Seawater samples were collected at the beginning of the experiment and after 1, 5 and 7 days. Nitrate concentrations were estimated by means of segmented flow analyzer QuAAtro 39 (Seal Analytical). Daily nitrate removal rates (NRR) were estimated in each incubation flask from the disappearance of nitrate after the first day of treatment. The NRR *vs.* initial nitrate concentration curve was fitted to the Michaelis-Menten model by non-linear least squares fitting. Maximal NRR (NRR_m) and semi-saturation concentration (K_m) were estimated from the fitting parameters.

The carbon and nitrogen contents of thallus pieces collected in the beach of Caleta (Tarifa) in February, March, June, July and August 2020 were determined. The total carbon and nitrogen contents of crude extracts were quantified using an elemental analyzer bounded to an IR detector CNHS LECO-932 (LECO Corp. MI, USA) by burning 10 mg of dry samples at 1000°C.

2.3. Statistical analyses

The weekly time series of air and water temperature and satellite chlorophyll *a* as well as the monhly time series of the modeled variables were analyzed by using the technique of seasonal decomposition. The seasonal, trend and irregular components of the time series were calculated with the function *Decompose* in R that performs a

classical seasonal decomposition by moving averages (Kendall and Stuart, 1983). Additionally, the daily time series of water temperature was used to analyze the frequency and intensity of extreme temperature events. The R package heatwaveR specifically designed to detect heatwaves and cold spells was used (Schlegel and Smit, 2018). The functions *ts2clm* and *detect_event* were used to detect duration and intensity of heatwave events defined as periods longer than four days for which the temperature was higher than the seasonally varying threshold value (90th percentile threshold; Hobday et al. 2016). The function *mcs* was used to detect cold spells defined as periods longer than four days for which temperature was lower than the seasonally varying 10th percentile threshold.

In order to research the changes in the hydro-geochemical patterns that occurred during the invasion, a principal component analysis (PCA) was performed with the monthly trend series of the variables obtained from the biogeochemical model of the E.U. Copernicus Marine Service. PCA permits identifying the main modes of variation of the hydro-geochemical variables as well as different time periods characterized by shifts in one or various variables. PCA run in R using the function *rda* of the package Vegan (Oksanen et al., 2014). The variables included in the analysis were temperature, salinity, transparency, nitrate, phosphate, chlorophyll *a*, mixed layer depth and velocity zonal and meridional components of the surface current. The variables were standardized prior to the analysis.

The differences in nutrient concentrations and salinity between coastal stations and the offshore station were tested with a Kluskal-Wallis test at $p<0.05$.

3. Results

3.1. Hydrology and nutrients

The weekly averaged time series showed maximal temperatures in air (26.5ºC) and water (22.8ºC) in July 2017 and July 2016, respectively. Concordantly, the temperature trend time series indicate that there was a warming period from 2015 to 2018 in both air and water (Fig. 2). Note that the intensity of this warming was smoother in water compared to air. Interestingly, the most extreme values of weekly temperature in water were obtained in winter and summer of 2016. The analysis of temperature extreme events based on the daily temperature time series indicates that there were 17 heatwave events in 2010-2020, 58% of which were produced during 2015-2019 (Suppl. Fig. 1) although the amount of days with heatwaves in 2015-2019 and 2010-2014 was similar. The longest heatwave was produced in 2010 while the most intensive heatwave was registered in 2016. The occurrence frequencies of cold spells in 2010-2014 and 2015-2019 were also similar. The most intensive cold spell occurred in 2015.

Satellite chlorophyll *a* in the study area averaged 0.3 μg L^{-1}, with annual peaks above 0.6 μg L^{-1} that were normally obtained in summer (Suppl. Fig. 2). However, it is remarkable that in 2015 and 2016, annual peaks of satellite chlorophyll *a* were not registered; in fact, the lowest weekly concentrations of chlorophyll *a* were obtained during these two annual periods when there was a decreasing trend compared to the rest of the time series.

The time series of the modeled variables indicate that hydrodynamic changed in the study area in 2015-2016 as surface salinity decreased and velocity zonal component increased in comparison to previous periods (Fig. 3; note that positive values of this

component indicate that the flow runs from west to east). The highest positive value in the irregular component time series of the zonal current velocity for the whole study period was produced in 2015. The outputs of the model also point out that surface nutrient concentrations increased in 2015, with annual maxima in 2016-2018 that were notably higher than the maxima modeled for previous years (Fig. 4).

The results of the PCA performed with the trend time series of the modeled variables also illustrate clearly these inter-annual changes. The first PC extracted (PC1) explained 43% of the variability (Fig. 5a). Transparency and meridional component of the current velocity were the most important variables that contributed positively to PC1 while nutrients and chlorophyll *a* did negatively. Therefore, this PC was related to changes in phytoplankton biomass which were associated to shifts in nutrient concentration and displacement velocity of the surface water from the north coast to the south. Salinity and current velocity zonal component were the main contributors to PC2 (20%) although the signs of the contributions were different. It can be assessed that this PC indicates changes in the horizontal transport velocity of the surface water masses that circulate throughout the Strait of Gibraltar. Note that temperature did not contribute to these two first variance components; however, this variable was the main contributor to PC3 (13% of explained variability) which indicates that part of the variability in the surface temperature trend series was not associated to hydrological variability. PC1 scores decreased progressively from 2010 to 2019 (Fig. 5b), which can be interpreted as higher nutrient concentration was associated to meridional current velocity decreasing. The variation time patterns of PC2 differed compared to PC1 given that the most negative scores were obtained in the period 2013-2017 indicating that the zonal current velocity increased during that period. It has to be noted that salinity and MLD were positively correlated to PC2 (Fig. 5c), therefore during that period of zonal current

velocity increasing, salinity and MLD reduced. Time series of the PC3 scores indicate that only a few monthly periods (roughly distributed every 3 years) contributed significantly to this PC from 2010-2014. However, it is notable that distribution of PC3 scores was more irregular since 2015, with some monthly periods presenting negative scores.

The variability in the concentrations of dissolved inorganic nitrogen (DIN) was higher in the coastal stations than in the offshore station (Fig. 6; note that there are not ammonium data available for open sea). Nitrate concentration averaged in the coastal stations ranged from 1.0 to 3.5 μM with the exception of 2017 when the average was lower than 0.7 μM. These yearly concentrations were higher than in the 20 m surface layer of the offshore station (apart of 2017) and similar to the concentrations in the offshore deeper layer. However, the nitrate maxima in the coast were notably higher than in the offshore deeper layer (Table 1) as also occurred with nitrite. Ammonium concentrations were fairly high in comparison to nitrate, especially in 2017 when the concentration maximum reached 20 μM. Phosphate concentrations at the coastal stations were less unstable than nitrate and similar to offshore. These data indicate that the coastal stations were enriched in DIN relative to phosphate in comparison to offshore. The nutrient concentrations varied irrespective of the salinity in the coastal stations (Suppl Fig. 3) where lower salinity was obtained in 2014 and 2015, matching the decreasing trend in modeled salinity (Fig. 3). In comparison to the offshore surface layer, the coastal stations had lower salinity.

3.2. Physiological features

The results of the nitrate removal experiments indicate that *R. okamurae* has high capacity for using dissolved inorganic nitrogen (Fig. 7a) as nitrate was almost

totally depleted after only one day of culture in the treatments with initial concentrations of 50 and 120 μM. In the treatments with the highest nitrate concentrations, nitrate removal followed a linear kinetic indicating that NRR kept roughly constant during the incubations. NRR calculated from removal after 24 h incubation followed saturation kinetics reaching the maximal rate at the highest concentration assayed (Fig. 7b). The semisaturation concentration (K_m) calculated by fitting these data to the Michaelis-Menten model was 135 μM and NRR at nitrate saturation (NRR_m) was 83 μmol N gFW^{-1} d^{-1}.

Carbon content of *R. okamurae* thalli collected in 2020 ranged from 34.2% in February to 42.1% in August. The lowest and highest N contents were obtained in June (1.4%) and August (4.5%), respectively. Consequently, the N content and C:N molar ratio in the algal tissue varied by about three-folds.

4. Discussion

4.1. Temperature, salinity and nutrient conditions in the Strait of Gibraltar

The presence of *Rugulopteryx okamurae* in macroalgal communities of the warm temperate western Pacific Ocean has been documented frequently (Hwang et al., 2009; Kitayama and Lin, 2012; Lim et al., 2017; Jung and Choi 2020; Jung et al., 2020). According to the published information, the alga grows in the shallow subtidal and above 15 m depth. In its native habitats, *R. okamurae* rarely becomes dominant; in fact, the maximal abundance reported in the literature is ca. 50 g FW m^{-2} and the highest coverage percentage is less than 5% (Jung and Choi, 2020; Jung et al., 2020; Lim et al., 2017). Consequently, the biomass and coverage reached by the alga in the SoG ($11 \cdot 10^3$

gFW m^{-2} and almost 100% of coverage in some points of Tarifa; García-Gómez et al., 2021) are indicative of growth rates not described before for this species in its natural habitat. Obviously, this sharp growth only can be attributable to features of the recipient environment which favor *R. okamurae* and/or are a detrimental to the native communities (Davidson et al., 2015). Increasing temperature is one of the environmental factors which would enhance the growth and competitive output of macroalgal invaders (Cebrián and Ballesteros, 2010; Martínez-Luscher and Holmer, 2010). Comparisons between the SoG and native habitats of *R. okamurae* (Table 1) indicate that, on average, maximal and mean temperatures in both areas are similar but the temperature winter minimum is higher in the SoG (14.0 ºC compared to 9.2 ºC; Jung and Choi, 2020; Jung et al., 2020; Lim et al., 2017). In its native habitat, *R. okamuare* is present round-year although its maximal growth rate is reached in spring-summer (Jung et al., 2020). The annual cycle of growth appears to be similar in the SoG (García-Gómez et al., 2021); however, warmer winters will imply that the active growth annual period of *R. okamurae* might be longer than in its native habitat (assuming that the temperature is a factor that regulates its annual cycle). In fact, significant growth of the alga has been described in Tarifa (northern SoG) even in winter (García-Gómez et al., 2018). Salinity also differs between the two areas; in the western Pacific Ocean, it varies within a reduced range below 34.5 while in the SoG salinity presents a wider variation range with minima above 34.9 and maxima frequently above 38.0 (Table 1). The sharp growth of *R. okamurae* in the SoG suggests that this species is euryhaline.

Nutrient regime in the SoG is characterized by presenting high variability linked to modifications in speed (from 0.05 ms^{-1} to 0.35 ms^{-1}) and/or entry angle of the strong and permanent eastwards current of the surface Atlantic Water (the so-called Atlantic Jet) that enters into the Alboran Sea (Sarhan et al., 2000; Sammartino et al.,

2015; Macias et al., 2016). Both, direction and strength of the flow (Sánchez-Garrido et al., 2013; Gómez-Jakobsen, 2019), influence significantly the surface circulation patterns, regulate the nutrient distribution and affect the productivity in the west side of the SoG (Sarhan et al., 2000, Reul et al. 2002, 2008). Furthermore, the Ekman transport favors upwellings of enriched waters in the own SoG (Macías et al., 2007), which are normally produced in Spring, when the phytoplankton annual bloom occurs (Ramírez et al., 2005). The highest nitrate concentrations in the surface waters are obtained under a certain combination of upwelling and tide cycle (Echevarría et al., 2002), contributing to increases in the N:Si:P ratio eastwards. However, the high DIN concentrations obtained in the coastal stations in our report (punctually higher than 20 μM) cannot be explained by hydrological variability. Furthermore, the phosphate concentration at these stations was low in comparison to DIN and the ratio DIN:P departed significantly from the molar ratio reported for SoG waters by Huertas et al. (2012). These results indicate that the study area is affected by important entries of nutrients from terrestrial sources as Mercado et al. (2018) suggested previously for the Bay of Algeciras based on data from 2012 to 2015. In the same sense, high concentrations of dissolved organic carbon produced by phytoplankton have been attributed to inputs from the rivers that flow in the west side of SoG, mainly the Guadalquivir river that receives enormous amount of agricultural leachate (Álvarez-Salgado et al., 2020). The increase in the zonal component of the velocity and reduction in the meridional component in 2016-2017 will imply that the inputs of terrestrial water from the Spanish coast will circulate closer to the northern coast. This change in the circulation pattern would contribute to local enrichment of the surface water in the coastal stations creating suitable conditions to stimulate the growth of *R. okamurae*.

4.2. Contribution of the physiological performance of R. okamurae *to the invasion*

High nutrient concentrations are prerequisite for macroalgal blooms as the bloom-forming species have nutrient assimilation elevated capacity compared to other algae (Wang et al., 2020). According to its kinetics of nitrate removal, irregular supply of high nutrients would give a competitive advantage to *Rugulopteryx okamurae* on native macroalgae. The high NRR_m is comparable with uptake rates reported for other bloom-forming macroalgae (Table 2) and implies that the alga will assimilate large amount of nitrate when the external concentrations are elevated. Nitrate affinity of *R. okamurae* is comparatively low taking into account values published for some of these bloom forming macroalgae (from 10 to 61 μM; see the data compiled in Wang et al. 2014). However, the relatively high K_m obtained in our experiments indicates that *R. okamurae* will respond to nitrate increases by linearly increasing its assimilation rates. Furthermore, this species will keep constants its nitrate removal rates for several days of growth under high nitrate unlike many other macroalgae that down-regulate the nitrate assimilation mechanisms (e.g. see den Hann et al., 2016 and Wang et al., 2014).

The growth responses to N supply depend on the interaction with the internal N pools; in fact, a relationship between ambient growth rates of *Ulva* spp. and thallus N content has been described (Fong et al., 2001; Teichberg et al., 2007). N content of *R. okamurae* was highly variable which would be indicative of storage capacity of N when its external supply is increased, which is also a common feature among bloom forming algae. For instance, it has been shown that the N internal pool of *U. lactuca* is linked to external DIN supply and can vary between 1.5% and 5.8% (Fujita, 1985; Pedersen and Borum, 1996; Teichberg et al., 2010). Furthermore, internally stored N would be used by the alga for keeping high growth rates when the external concentrations decrease

(Lartigue and Sherman, 2006; Kennison et al., 2011). The fact of C content in *R. okamurae* is high regardless of its N content, would be indicative of high carbon fixation rates are reached even under low DIN concentrations, which is expected if the alga uses internal N. Compared to macroalgae inhabiting rocky areas of the southern Iberian Peninsula (collected close to the study area; see Mercado et al., 2009, for a more detailed description), *R. okamuare* presented the highest C content (Suppl. Fig. 4). It is also notable that the variation range of N content covered the whole range reported for the macroalgae with N content higher than 1% collected at the southern Iberian Peninsula. This variability in N content is consistent with the great morphological plasticity that has been described for *R. okamurae* not only in the SoG (Figueroa et al., 2020; Salido and Altamirano, 2020; García-Gómez et al., 2021) but also in its origin place (Hwang et al., 2009). Note that physiological plasticity is a common characteristic of the invasive algae (Davidson et al., 2015; Zanolla et al., 2019) which permits their opportunistic growth when the external conditions are favorable.

It cannot be discarded that the changing hydrological conditions described in our report also affected negatively the native communities. Thus, it is notable that 2016 was the annual period with the most extreme temperatures (including the occurrence of an intensive waveheat event) and that the winters of 2017-2018 were particularly warmer. Furthermore, modeled salinity for this period decreased notably. It is possible that these environmental changes decreased the competitive performance of the native communities. Furthermore, the hydrological changes that occurred before the massive presence of *R. okamurae* in 2016 could reduce the resilience capacity of the ecosystem although damages on native communities were not registered prior the invasion (García-Gómez et al., 2021).

In summary, our data indicate that the success of *R. okamurae* in the SoG could be due to a combination of both its particular physiological characteristics and the favorable environmental conditions for its growth, including the high DIN availability possibly being discharged from terrestrial sources. At any rate, more research on the eco-physiology of the alga is necessary to assess its invasive capacity which would be not only based on its response to seasonal and short-term changes in temperature, salinity and nutrients but also on biotic factors. For instance, recently Casal-Porras et al. (2021) have shown that *R. okamurae* presents high dilkamural content , a toxic compound for native herbivores. The surface circulation associated to the Atlantic jet entering into the Alboran Sea (García Lafuente et al., 2000; Gómez-Jakobsen, 2019) might favor the fast expansion and colonization of nearby coastal areas. Additionally, the fishery activity is elevated in the Spanish coast, particularly the bottom trawling fishing (Muñoz et al., 2018) which would pluck *R. okumare* and contribute to its spread along the coast. Therefore, this species should be closely monitored in the southern Europe.

Acknowledgements

The analyses were supported by the project 10-ESMARES2-C4A2 (financed by Spanish Ministry of Ecological Transition and Demographic Challenge), the project UMA18-FEDERJA162 (financed by FEDER Andalucía 2014-2020), Project Blue Maro PID2020-116136RB-I00 financed by the Ministry of Science and Innovation of Spanish Government and the research groups RNM295 and RNM338 (Junta de Andalucía). BB acknowledges funding from a fellowship of CAPES/PRINT Program, Process n. 88887.374403/2019-00. We thank the Spanish Meteorological Agency (AEMET) for providing data.

Credit Author Statement

Mercado JM: conceptualization, writing, original draft, data collection and analysis; **Gómez-Jakobsen F**: satellite and meteorological data collection, time series analysis, review; **Avilés A:** analysis of nutrients, nutrient data collection, review and editing; **Bonomi-Barufi J**: sample collection, design and performing of lab experiments, review and editing; **Muñoz M:** conceptualization, modelled data collection, review and editing; **Reul A:**conceptualization, modelled data collection, review and editing; **Korbee N:** sample collection, design and performing of lab experiments, review and editing; **Figueroa FL:** conceptualization, writing, review and editing, sample collection and lab analysis.

References

Altamirano-Jeschke, M., De la Rosa Álamos, J., Martínez-Medina, F.J., 2016. Arribazones de la especie exótica *Rugulopteryx okamurae* (E.Y. Dawson) I.K. Hwang, W.J. Lee & H.S. Kim (Dictyotales, Ochrophyta) en el Estrecho de Gibraltar: primera cita para el Atlántico y España. Algas 52, 20.

Álvarez-Salgado, X.A., Oter, J., Flecha, S., Huertas, I.E., 2020. Seasonality of dissolved organic carbone xchange across the Strait of Gibraltar. Geoph. Res. Lett. 47. https://doi.org/10.1029/ 2020GL089601.

Azmi, F., Primo, C., Hewitt, C.L., Campbell, M.L., 2015. Assessing marine biosecurity risks when data are limited: bioregion pathway and species-based exposure analyses. ICES J. Mar. Sci. 72, 1078-1091. https://doi.org/10.1093/icesjms/fsu236.

Bambaranda, B.V.A.S.M., Susaka, T.W., Chirapart, A., Salin, K.R., Sasaki, N., 2019. Capacity of *Caulerpa lentillifera* in the removal of fish culture effluent in a recirculating aquaculture system. Processes 7, 440, https://doi.org/10.3390/pr7070440.

Boudouresque, C.F., Verlaque, M., 2002. Biological pollution in the Mediterranean Sea: invasive versus introduced macrophytes. Mar. Pollut. Bull. 44, 32-38. https://doi.org/10.1016/S0025-326X(01)00150-3.

Boudouresque, C.F., Verlaque, M., 2005. Nature conservation, Marine Protected Areas, suitable development and the flow of invasive species to the Mediterranean Sea. TR Scient. Parc. Nat. de Port-Cros 21, 29-54.

Boudouresque, C.F., Klein, J., Ruitton, S., Verlaque, M., 2011. Biological invasions: The Thau lagoon, a Japanese biological island in the Mediterranean Sea. In: Global Change: Mankind-Marine Environmental Interactions; Ceccaldi, H.J., Girault, I., Stora, G., Eds. Springer Publisher: Dordrecht, The Netherlands. pp. 151-156.

Casal-Porras, I., Zubía, E., Brun, F.G., 2021. Dilkamural: A novel chemical weapon involved in the invasive capacity of the alga *Rugulopterux okamurae* in the Strait of Gibraltar. Est. Coastal Shelf. Sci. 257, 107398. https://doi.org/10.1016/j.ecss.2021.107398.

Cebrián, E., Ballesteros, E., 2010. Invasion of Mediterranean benthic assemblages by red alga *Lophocladia lallemandii* (Montagne) F. Schmitz: Depth-related temporal variability in biomass and phenology. Aquatic Bot. 92, 81-85. https://doi.org/10.1016/j.aquabot.2009.10.007.

Chávez, V., Uribe-Martínez, A., Cuevas, E., Rodríguez-Martínez, R.E., van Tussenbroek, B.I., Francisco, V., Estévez, M., Celis, L.B., Monroy-Velázquez, L.V., Leal-Bautista, R., Álvarez-Filip, L., García-Sánchez, M., Masia, L., Silva, R., 2020. Massive influx of pelagic *Sargassum* spp. on the coasts of the Mexican Caribbean 2014–2020: Challenges and opportunities. Water 12, 2908. https://doi.org/10.3390/w12102908.

Dailer, M.L., Smith, J.E., Smith, C., 2012. Responses of bloom forming and non-bloom forming macroalgae to nutrient enrichment in Hawai'i, USA. Harmful Algae 17, 111-125, https://doi.org/125. 10.1016/j.hal.2012.03.008.

498 Davidson, A.D., Campbell, M.L., Hewitt, C.L., Schaffelke, B., 2015. Assessing the
499 impacts of non indigenous marine macrogalgae: an update of current knowledge.
500 Bot. Mar. 58, 55-79, https://doi.org/10.1515/bot-2014-0079.
501 den Hann, J., Huisman, J., Brocke, H.J., Goehlich, H., Latijnhouwers, K.R.W., van
502 Heeringen, S., Honcoop, S.A.S., Bleyenberg, T.E., Schouten, S., Cerli, C.,
503 Hoitinga, L., Vermeij, M.J.A., Visser, P.M., 2016. Nitrogen and phosphorus uptake
504 rates of different species from a coral reef community after a nutrient pulse. Sci.
505 Rep. 6, 28821. https://doi.org/10.1038/srep28821.
506 DeClerck, L., Leliaert, F., Verbruggen, H., Lane, C.E., DePaula, J.C., Payo, D.I.,
507 Coppejans, E., 2006. A revised classification of thw Dictyoteae (Dictyotales,
508 Phaeophyceae) based on rbcL and 26S ribosomal DNA sequence data analyses. J
509 Phycol. 42, 1271-1288. https://doi.org/10.1111/j.1529-8817.2006.00279.x.
510 Diez, J.M., D'Antonio, C.M., Dukes, J.S., Grosholz, E.D., Olden, J.D., Sorte, C.J.B.,
511 Blumenthal, D.M., Bradley, B.A., Early, R., Ibáñez, I., Jones, S.J., Lawler, J.J.,
512 Miller, L.P., 2012. *Will extreme climatic events facilitate biological invasions?*
513 Front. Ecol. Environ. 10, 249–257. https://doi.org/10.1890/110137.
514 Echevarría, F., García Lafuente, J., Bruno, M., Gorsky, G, Goyx, M., González, N.,
515 Garía, C.M., Gómez, F., Vargas, J.M., Picheral, M., Stirby, L., Varela, M., Alonso,
516 J.J., Reul, A., Cózar, A., Prieto, L., Sarhan, T., Plaza, F., Jiménez-Gómez, F. 2002.
517 Physical-biological coupling in the Strait of Gibraltar. Deep-Sea Res. II 49, 4115-
518 4130. https://doi.org/10.1016/S0967-0645(02)00145-5.
519 El Aamri, F., Idhalla, M., Tamsouri, M.N., 2018. Occurrence of the invasive brown
520 seaweed *Rugulopteryx okamurae* (E.Y.Dawson) I.K.Hwang. J.Lee H.S. Kim
521 (Dictyotales. Phaeophyta) in Marocco (Mediterranean Sea). Mediterranean Fish.
522 Aqu. Res. 1, 92-96.

523 Faria, J., Prestes, C.L., Moreu, I., Martins, I.G., Neto, A.I., Cacabelos, E., 2021. Arrival
524 and proliferation of the invasive seaweed *Rugulopteryx okamurae* in NE Atlantic
525 islands. bioRxiv. https://doi.org/10.1101/2021.06.25.448933.
526 Figueroa, F.L., Vega, J., Gómez-Valderrama, M., Korbee, N., Mercado, J.M., Bañares,
527 E., Flores-Moya, A., 2020. Invasión de la especie exótica *Rugulopteryx okamurae*
528 en Andalucía I: estudios preliminares de la actividad fotosintética. Algas 56, 35-46
529 Fong, P., Kramer, K., Boyer, K.E., Boyle, K.A., 2001. Nutrient content of macroalgae
530 with differing morphologies may indicate sources of nutrients for tropical marine
531 systems. Mar. Ecol. Prog. Ser. 220, 137-152. https://doi.org/10.3354/meps220137.
532 Franks, J., Johnson, D., Ko, D., 2016. Pelagic *Sargassum* in the Tropical North Atlantic.
533 Gulf Caribb. Res.27, SC6–SC11. https://doi.org/10.18785/gcr.2701.08.
534 Fujita, R.M., 1985. The role of nitrogen status in regulating transient ammonium uptake
535 and nitrogen storage by macroalgae. J. Exp. Mar. Biol. Ecol. 92, 283-301.
536 https://doi.org/10.1016/0022-0981(85)90100-5.
537 García-Gómez, J.C., Sempere-Valverde, J., Ostalé-Valriberas, E., Martínez, M., Olaya-
538 Ponzone, L., González, A.R., Espinosa, F., Sánchez-Moyano, E., Megina, C.,
539 Parada, J.A., 2018. *Rugulopteryx okamurae* (EY Dawson) IK Hwang, WJ Lee &
540 HS Kim (Dictyiotales, Ochrophyta), alga exótica "explosiva" en el estrecho de
541 Gibraltar. Observaciones preliminares de su distribución e impacto. Almoraima 48,
542 97-113.
543 García-Gómez, J.C, Florido, M., Olaya-Ponzone, L., Rey Díaz de Rada, J., Donázar-
544 Aramendía, I., Chacón M., Quintero J., Magariño S., Megina, C., 2021. Monitoring
545 extreme impacts of *Rugulopteryx okamurae* (Dictyotales, Ochrophyta) in El
546 Estrecho Natural Park (Biosphere Reserve). Showing radical changes in the
547 underwater seascape. Front. Ecol. Evol. https://doi.org/10.3389/fevo.2021.639161.

García-Lafuente, J., Vargas, J.M., Plaza, F., Sarhan, T., Candela, J., Bascheck, B., 2000. Tide at the eastern section of the Strait of Gibraltar. J. Geophy. Res. 105:14197-14213. https://doi.org/10.1029/2000JC900007.

Gennaro, P., Piazzi, L., 2014. The indirect role of nutrients in enhancing the invasion of *Caulerpa racemosa* var *cylindracea*. Biol. Invasions 16, 1709-1717. https://doi.org/10.1007/s10530-013-0620-y.

Gómez, F., Gorsky, G., Garcia-Gorriz, E., Picheral, 2004. Control of phytoplankton distribution in the Strait of Gibraltar by wind and fortnightly tides. Estuar. Coast. Shelf Sci. 59, 85–497. https://doi.org/10.1016/j.ecss.2003.10.008.

Gómez-Jakobsen, F.J., Mercado, J.M., Tovar-Salvador, M.L., Cortés, D., Yebra, L., Salles, S., Sánchez, A., Valcárcel-Pérez, N., Alonso, A., 2018. New algorithms for estimating chlorophyll-*a* in the Spanish waters of the Western Mediterranean Sea from multiplatform imagery, Int. J. Remote Sensing, 39, 23. 8837-8858, https://doi.org/10.1016/j.ecss.2019.05.012.

Gómez-Jakobsen, F.J., Mercado, J.M., Cortés, D., Yebra, L., Salles, S., 2019. A first description of the summer upwelling off the Bay of Algeciras and its role in the northwestern Alboran Sea. Est. Coast. Shelf Sci. 225, 106230. https://doi.org/10.1016/j.ecss.2019.05.012.

Gordillo, F.J.L., Figueroa, F.L., Niell, F.X., 2001. Non-photosynthetic enhancement of growth by high CO_2 level in the nitrophilic seaweed *Ulva rigida* C. Agardh (Chlorophyta). Planta 213, 64-70. https://doi.org/10.1007/s004250000468.

Gordillo, F.J.L., Dring, M., Savidge, G., 2002. Nitrate and phosphate uptake characteristics of three species of brown algae cultured at low salinity. Mar. Ecol. Prog. Ser. 234, 110-118. https://doi.org/10.1007/s004250000468.

572 Hobday, A.J., Alexander, L.V., Perkins, S.E., Smale, D.A., Straub, S.C., Oliver, E.C.J.,
573 Benthyysen, J.A., Burrows, M.T., Donat, M.G., Feng, M., Holbrook, N.J., Moore,
574 P.J., Scannell, H.A., Gupta, A.S., Wernberg, T., 2016. A hierarchical approach to
575 defining marine heatwaves. Prog. Oceanog. 141, 227-238. doi:
576 10.1016/j.pocean.2015.12.014.
577 Huertas, I.E., Rós, A.F., García Lafuente, J., Navarro, G., Makouni, A., Sánchez-
578 Román, A., Rodríguez-Gálvez, S., Orbi, A., Ruiz, J., Pérez, F.F., 2012. Atlantic
579 forcing of the Mediterranean oligotrophy. Global Biogeochem. Cycles 26, GB2022.
580 https://doi.org/10.1029/2011GB004167.
581 Hwang, I-K., Lee, W.J., Kim H.-S., De Clerck, O., 2009. Taxonomic reappraisal
582 of *Dilophus okamurae* (Dictyotales, Phaeophyta) from the western Pacific
583 Ocean. Phycologia 48, 1-12. https://doi.org/10.2216/07-68.1.
584 Jung, S.-W., Choi, C.-G., 2020. Characteristics of marine algal communities in the
585 Spring at Gijang-gun, Busan. J. Kor. Soc. Mar. Environ. Saf., 26, 178-185.
586 https://doi.org/10.7837/kosomes.2020.26.2.175.
587 Jung, S.-W., Rho, H.S., Choi, C.G., 2020. Characteristics and ecosystems changes of
588 marine algal communities in Wangdol-cho on the East coast of Korea. Ocean Sci. J.
589 55, 549-562. https://doi.org/10.1007/s12601-020-0034-6.
590 Kendall, M., Stuart, A., 1983. The advanced Theory of Statistics, Vol3, Griffin, pp.410-
591 414.
592 Kennison, R.L., Kamer, K., Fong, P., 2011. Rapid nitrate uptake rates and large short-
593 term storage capacities may explain why opportunistic green macroalgae dominate
594 shallow eutrophic stuaries. J. Phycol. 47, 483-494, https://doi.org/10.1111/j.1529-
595 8817.2011.00994.x.

596 Kitayama, T., Li, S.-M., 2012. Brown algae from Chaojing, Keelung, City, Taiwan.
597 Mem. Natl. Mus. Nas. Sci. Tokyo 48, 149-157.
598 Kraan, S., 2016. *Undaria* marching on; late arrival in the Republic of Ireland. J Appl
599 Phycol. https://doi.org/10.1007/s10811-016-0985-2.
600 Lapointe, B.E., Bedford, B.J., 2011. Storm water nutrients inputs favor growth of non-
601 native macroalgae (Rhodophyta) on O'ahu Hawaiian Islands. Harmful Algae 10,
602 310-318. https://doi.org/10.1016/j.hal.2010.11.004.
603 Lartigue, J., Sherman, T.D., 2006. A field study of nitrogen storage and nitrate
604 reductase activity in the estuarine macroalgae *Enteromorpha lingulata*
605 (Chlorophyceae) and *Gelidium pusillum* (Rhodophyceae). Stuaries Coasts 29, 699-
606 708. https://doi.org/10.1007/BF02784294.
607 Lim, S.Y., Kang, M.-G., Lee, C.H., Kim, S.J., Shin, J.-A., 2017. A spring algal
608 vegetation in the Muan, Jindo and Geomundo Coast, Western South Sea of Korea.
609 J. Fish. Mar. Sci. 29, 612-625. https://doi.org/10.13000/JFMSE.2017.29.2.612.
610 Macías, D., Martín, A.P., García-Lafuente, J., García, C.M., Yool, A., Bruno, M.,
611 Vázquez-Escobar, A., Izquierdo, A., Sein, D.V., Echeverría, F., 2007. Mixing and
612 biogeochemical effects induced by tides on the Atlantic-Mediterranean flow in the
613 Strait of Gibraltar. An analysis through a physical-biological coupled model. Prog.
614 Oceanogr. 74, 252– 272. https://doi.org/doi:10.1016/j.pocean.2007.04.006.
615 Macias, D., Garcia-Gorriz, E., Stips, A., 2016. The seasonal cycle of the Atlantic Jet
616 dynamics in the Alboran Sea: Direct atmospheric forcing versus Mediterranean
617 thermohaline circulation. Ocean Dyn. 66, 137– 151.
618 https://doi.org/doi:10.1007/s10236-015-0914-y.

Martínez-Lüscher, J., Holmer, M., 2009. Potential effects of the invasive species *Gracilaria vermiculophylla* on *Zostera marina* metabolism and survival. Mar. Env. Res. 69, 345-349. https://doi.org/10.1016/j.marenvres.2009.12.009.

Meinesz, A., de Vaugelas, J., Hesse, B., Mari, X., 1993. Spread of the introduced tropical green alga *Caulerpa taxifolia* in northern Mediterranean waters. J. Appl. Phycol. 5**,** 141.

Meinesz, A., Belsher, T., Thibaut, T. et al. 2001. The introduced green alga *Caulerpa taxifolia* continues to spread in the Mediterranean. Biological Invasions 3, 201–210. https://doi.org/10.1023/A:1014549500678.

Mercado, J.M., Gordillo, F.J.L., Figueroa, F.L., Niell, F.X., 1999. Effects of different level of CO_2 on photosynthesis and cell components of the red alga Porphyra leucosticta. J. Appl. Phycol. 11, 455-461. https://doi.org/10.1023/A:1008194223558.

Mercado, J.M., de los Santos, C.B., Pérez-Lloréns, L., Vergara, J.J., 2009. Carbon isotopic fractionation in macroalgae from Cádiz Bay (Southern Spain): Comparison with other bio-geographic regions. Est. Coastal Shelf Sci. 85, 449-458. https://doi.org/doi:102290/w10070938.

Mercado, J.M., León, P., Salles, S., Cortés, D., Yebra, L., Gómez-Jakobsen, F., Herrera, I., Alonso, I., Sánchez, A., Valcárcel-Pérez, N., Putzeys, S., 2018. Time variability patterns of eutrophication indicators in the Bay of Algeciras (South Spain). Waters 10, 938. https://doi.org/doi:102290/w10070938.

Meretta, P.E., Matula, C., Casas, G., 2012. Occurrence of the alien kelp *Undaria pinnatifida* (Laminariales, Phaeophyceae) in Mar del Plata, Argentina. BioInvasions Records 1, 59-63. https://doi.org/10.3391/bir.2012.1.1.13.

643 Muñoz, M, Reul, A., Gil de Sola, L., Lauerburg, R.A.M., Tello O., Gimpel, A.,
644 Stelzenmüller V., 2018. A spatial risk approach towards integrated marine spatial
645 planning: A case study on European hake nursery areas in the North Alboran Sea.
646 Mar. Env. Res. 142, 190-207. https://doi.org/10.1016/j.marenvres.2018.10.008.
647 Noè, S., Badalamenti, F., Bonaviri, C., Musco, L., Fernández, T.V., Vizzini, S.,
648 Gianguzz, P., 2018. Food selection of a generalist herbivore exposed to native and
649 alien seaweeds. Mar. Pollution Bull., 129, 469-473.
650 Oksanen, J., Blanchet, F.G., Kindt, R., Legendre, P., Minchin, P.R., O'Hara, R.B.,
651 Simpson, G.L., Solymos, P., Stevens, M.H.H. and Wagner, H., 2014. Vegan:
652 Community Ecology Package. R Package Version 2.2-0.
653 Pedersen, M.F., Borum, J., 1996. Nutrient control of algal growth in the esturarine
654 waters. Nutrient limitation and the importance of nitrogen requirements and
655 nitrogen storage among phytoplankton and species macroalgae. Mar. Ecol. Prog.
656 Ser. 142, 261-272.
657 Piazzi L., Ceccherelli G., Cinelli F., 2001. Threat to macroalgal diversity: effects of the
658 introduced green alga *Caulerpa racemosa* in the Mediterranean. Mar. Ecol. Prog.
659 Ser. 210, 149-159.
660 Piazzi L., Cinelli F., 2003. Evaluation of benthic macroalgal invasion in a harbour area
661 of the western Mediterranean Sea. Eur. J. Phycol. 38, 223-231.
662 https://doi.org/10.1080/1364253031000136358.
663 Piazzi L., Meinesz A., Verlaque M., Akcali B., Antolic B., Argyrou M., Balata D.,
664 Ballesteros E., Calvo S., Cinelli F., Cirik S., Cossu A., 2005. Invasion of *Caulerpa*
665 *racemosa* var. cylindracea (Caulerpales, Chlorophya) in the Mediterranean Sea: An
666 assesment of the spread. Crygtogamie Algologie 26, 189-202.

667 Piazzi L., Balata D., 2009. Invasion allien macroalgae in different Mediterranean
668 habitats. Biol Invasions 11, 193-204.
669 Piazzi, L., Balata, D., Bulleri, F., Gennaro, P., Ceccherelli, G., 2016. The invasion of
670 *Caulerpa cylindracea* in the Mediterranean: the know, unknown and the knowable.
671 Mar. Biol. 163, 161. doi: 10.1007/s00227-016-2937-4.
672 Ramírez, T., Cortés, D., Mercado, J.M., Vargas-Yañez, M., Sebastián, M., Liger, E.,
673 2005. Seasonal dynamics of inorganic nutrients and phytoplankton in the NW
674 Alboran Sea. Est. Coast. Shelf Res. 65, 654-670.
675 https://doi.org/10.1016/j.ecss.2005.07.012.
676 Reul, A., Vargas, J.M., Jiménez-Gómez, F., Echevarría, F., García-Lafuente, J.,
677 Rodríguez, J., 2002. Exchange of planktonic biomass through the Strait of Gibraltar
678 in late summer conditions. Deep Sea Res. Part II 49, 4131-4144.
679 https://doi.org/10.1016/S0967-0645(02)00146-7.
680 Reul, A., Rodríguez, J., Guerrero, F., González, N., Vargas, J. M., Echevarría, F.,
681 Jimenéz-Gómez, F., 2008. Distribution and size biomass structure of
682 nanophytoplankton in the Strait of Gibraltar. Aquat. Microb. Ecol. *52*, 253–262.
683 https://doi.org/10.3354/ame01217.
684 Ribera Siguan, M.A., 2002. Review of non-native marine plants in the Mediterranean
685 Sea. In Leppäkoski E, Gollasch S, Olenin S(eds), Invasive Aquatic Species of
686 Europe. Distribution, Impacts and Management. Kluwer Academic Publishers,
687 Dordrecht, pp. 291–310.
688 Ruitton, S., Blanfuné, A., Boudouresque, C.-F., Guillemain, D., Michotey, V., Roblet,
689 S., Thibault, D., Thibaut, T., Verlaque, M., 2021. Rapid Spread of the Invasive
690 Brown Alga *Rugulopteryx okamurae* in a National Park in Provence (France,
691 Mediterranean Sea). Water 13, 2306. https://doi.org/10.3390/ w13162306.

692 Salido, M., Altamirano, M., 2020. Variabilidad temporal de la morfología e invasividad
693 de *Rugulopteryx okamurae* (Dictyotales, Ochrophyta) en el estrecho de Gibraltar.
694 Algas, 56, 101.
695 Sammartino, S., García-Lafuente, J., Naranjo, C., Sánchez-Garrido, J.C., Sánchez-
696 Leal, R., Sánchez-Román, A., 2015. Ten years of marine current measurements
697 in Espartel sill, Strait of Gibraltar, J. Geophys. Res.: Oceans 120, 6309-6328,
698 http://dx.doi.org/10.1002/2014JC010674.
699 Sánchez-Garrido, J.C., García-Lafuente, J., Álvarez-Fanjul, E., Sotillo, M.G., de
700 los Santos, F., 2013. What does cause the collapse of the Western Alborán
701 Gyre? Results of an operational model. Prog. Oceanogr., 116, 142-153.
702 http://dx.doi.org/10.1016/j.pocean.2013.07.002.
703 Sarhan T, García-Lafuente J, Vargas M., Vargas, J.M., Plaza, P., 2000. Upwelling
704 mechanisms in the northwestern Alboran Sea. J. Mar. Syst.23,317–31.
705 https://doi.org/10.1016/S0924-7963(99)00068-8.
706 Scheibling, R.E., Gagnon, P. 2006. Competitive interactions between the invasive green
707 alga *Codium fragile* ssp. *tomentosoides* and native canopy-forming seaweeds in
708 Nova Scotia (Canada). Mar. Ecol. Prog. Ser. 325,1-14.
709 https://doi.org/10.3354/meps325001.
710 Shaffelke, B., Smith, J.E., Hewitt, C.L., 2006. Introduced Macroalgae – a Growing
711 Concern. J. Appl. Phycol. 18, 529-541. https://doi.org/10.1007/s10811-006-9074-2.
712 Schlegel, R.W., Smit, A.J., 2018. heatwaveR: A central algorithm for the detection of
713 heatwaves and cold-spells. J. Open Source Sofware. 3(27), 821.
714 doi:10.21105/joss.0081.
715 Teichberg, M., Heffner, L., Fox, S., Valiela, I., 2007. Nitrate reductase and glutamine
716 synthetase activity, internal N pools, and growth of *Ulva lactuca*: responses to long

717 and short-term N supply. Mar. Biol., 151, 1249-
718 1259. https://doi.org/10.1007/s00227-006-0561-4.
719 Teichberg, M., Fox, S.E., Olsen, Y.S., Valiela, I., Martinetto, P., Iribarne, O., Muto,
720 E.Y., Petti, M.A.V., Corbisier, T.N., Soto-Jiménez, M., Páez-Osuna, F., Castro, P.,
721 Freitas, H., Zitelli, A., Cardinaletti, M., Tagliapietra, D., 2010. Eutrophication and
722 macroalgal blooms in temperate and tropical coastal waters: nutrient enrichment
723 experiments with *Ulva* spp. Global Change Biol. 16, 2624-2637.
724 https://doi.org/10.1111/j.1365-2486.2009.02108.x.
725 Verlaque, M., Fritayre, P., 1994. Modifications des communautés algales
726 méditerranéennes en présence de l'algue envahissante Caulerpa taxifolia (Vahl) C.
727 Agardh. Oceanologica Acta 17, 659-672.
728 https://archimer.ifremer.fr/doc/00099/21018/.
729 Verlaque, M., Steen, F., De Clerck, O. 2009. *Rugulopteryx* (Dictyotales,
730 Phaeophyceae), a genus recently introduced to the Mediterranean. Phycologia 48,
731 536-542. https://doi.org/10.2216/08-103.1.
732 Vermeij, M.J.A., Smith, T.B., Dailer, M.L., Smith, C.M., 2009. Release from native
733 herbivores facilities the persitence of invasive marine algae: a biogeographial
734 comparison of the relative contribution of nutrients and herbivory to invasion
735 success. Biol invasions 11, 1463-1474.
736 Wang, C., Lei, A., Zhou, K., Hu, Z., Hao W.,Yang, J., 2014. Growth and nitrogen
737 uptake characteristics reveal outbreak mechanism of the opportunistic macroalga
738 *Gracilaria tenuisipitata*. PloS ONE 9(10): e108980.
739 https://doi.org/doi:10.1371/journal.pone.0108980.

Wang, M., Hu, C., Barnes, B.B., Mitchum, G., Lapointe, B., Montoya, J.P., 2019. The great Atlantic *Sargassum* belt. Science 365, 83. https://doi.org/10.1126/science.aaw7912.

Wang, H., Wang, G., Gu, W., 2020. Macroalgal blooms caused by marine nutrient changes resulting from human activities. J. Appl. Phycol. 57, 766-776. https://doi.org/10.1126/science.aaw7912.

Williams, S.L., Smith, J.E., 2007. A global review of the distribution, taxonomy, and impacts of introduced seaweeds. Ann. Rev. Ecol. Evol. Syst. 38, 327–359. https://doi.org/10.1146/annurev.ecolsys.38.091206.095543.

Zanolla, M., Carmona, R., Kawai, H., Stengel, D.B., Altamirano, M. 2019. Role of thermal photosynthetic plasticity in the dispersal and settlement of two global green tide formers: *Ulva pertusa* and *U. ohnoi*. Mar. Biol. 166, 123. https://doi.org/10.1007/s00227-019-3578-1.

Zenetos, A., Galanidi, M. 2020. Mediterranean non indigenous species at the start of the 2020s: recent changes. Marine Biodiversity Records 13. https://doi.org/10.1186/s41200-020-00191-4.

Zhao, J., Jiang, P., Qiu, R.,Ma, Y., Wu, C., Fu, H., Chen, H., Li, F., 2019. The Yellow Sea green tide: A risk of macroalgae invasion. Harmful algae 77, 11-17. https://doi.org/10.1016/j.hal.2018.05.007.

Zhang, Q.-C., Yu, R.-C., Chen, Z.F., Qiu, L.M., Wang, Y.-F., Kong, F.Z., Geng, H.-X., Zhao, Y., Jiang, P., Yan, T., Zhou, M.-J., 2018. Genetic evidence in tracking the origin of *Ulva prolifera* blooms in the Yellow Sea, China. Harmful Algae 78, 86-94. https://doi.org/10.1016/j.hal.2018.08.002.

766

767 **Table 1.** Means of temperature and nutrient concentrations measured in coastal stations
768 close to Tarifa for different time periods within 2010-2019. Maximum and minimum
769 values are also shown. 'Natural habitats' indicate the values of temperature and salinity
770 published in the literature for the growth native area of *Rugulopteryx okamurae*.

		2010-2014	**2015-2016**	**2017-2019**	**Native habitats**
T air (ºC)	mean	17.5	18.8	18.0	-
	max	25.5	26.0	26.5	-
	min	9.3	10.9	9.4	-
T water (ºC)	mean	17.1	17.4	17.2	17.1
	max	21.6	22.8	21.3	23.8
	min	14.1	14.0	14.8	9.2
Salinity	mean	36.34	36.57	36.03	-
	max	37.96	38.04	36.97	34.30
	min	34.92	35.33	35.26	33.15
Nitrate (μM)	mean	2.14	1.94	1.28	-
	median	1.81	1.50	1.14	-
	max	6.39	5.52	3.92	
	SD	1.80	1.50	1.61	
Nitrite (μM)	mean	0.40	0.29	0.27	-
	median	0.22	0.30	0.24	-
	max	4.13	0.72	0.93	-
	SD	0.66	0.05	0.06	-
Ammonium (μM)	mean	1.24	0.99	2.82	-
	median	0.35	0.87	1.30	-
	max	8.06	2.71	20.2	-
	SD	1.63	0.52	4.60	-
Dissolved inorganic nitrogen (μM)	mean	3.74	3.21	4.37	-
	median	2.88	2.79	2.73	-
	max	13.14	8.35	23.09	-
	SD	2.91	1.78	5.17	-
Phosphate (μM)	mean	0.08	0.12	0.08	-
	median	0.05	0.07	0.05	-
	max	0.45	0.58	0.20	-
	SD	0.06	0.13	0.05	-

771

772

773

774 **Table 2.** Rates of nitrate removal (NRR) published for different macroalgae including
775 some bloom-former species (only data expressed on fresh weight basis have been
776 considered). The experimental conditions are indicated (T: temperature; I: μmol photons
777 m^{-2} s^{-1}; P: photoperiod).

	NRR [μmoles $gFW^{-1}d^{-1}$]	**Experimental Conditions**	**Source**
R. okamurae	83	T: 25ºC; I: 250;P: 12:12	This work
Porphyra leucosticta	43	T: 15ºC; I: 60; P: 12:12	Mercado et al. 1999
Fucus vesiculosis	10	T: 15ºC; I: 100;P: 10:14	Gordillo et al. 2002
Fucus serratus	10		
Laminaria digitata	10		
Ulva lactuca	150	T: 25ºC; I: 100; P: 12:12	Gordillo et al. 2001
Achantaphora spicifera	42.4	Outdoor conditions	Dailer et al. 2012
Dictyota acutiloba	50.6		
Hypnea musciformis	24.9		
Ulva lactuca	28.5		
Caulerpa lentillifera	150	T: 27ºC; I: 150; P: 12:12	Bambaranda et al. (2019)

778

779

Fig. 1. Position of the meteorological station (TARIFA-METEO), underwater probe of temperature (TARIFA BUOY), sampling coastal stations where nutrient data were obtained (solid black squares) and open sea station (ALGECIRAS). The coordinates of the locations from which modeled (IBI-MODEL) and satellite data (SMED-CHLA) were retrieved are also shown.

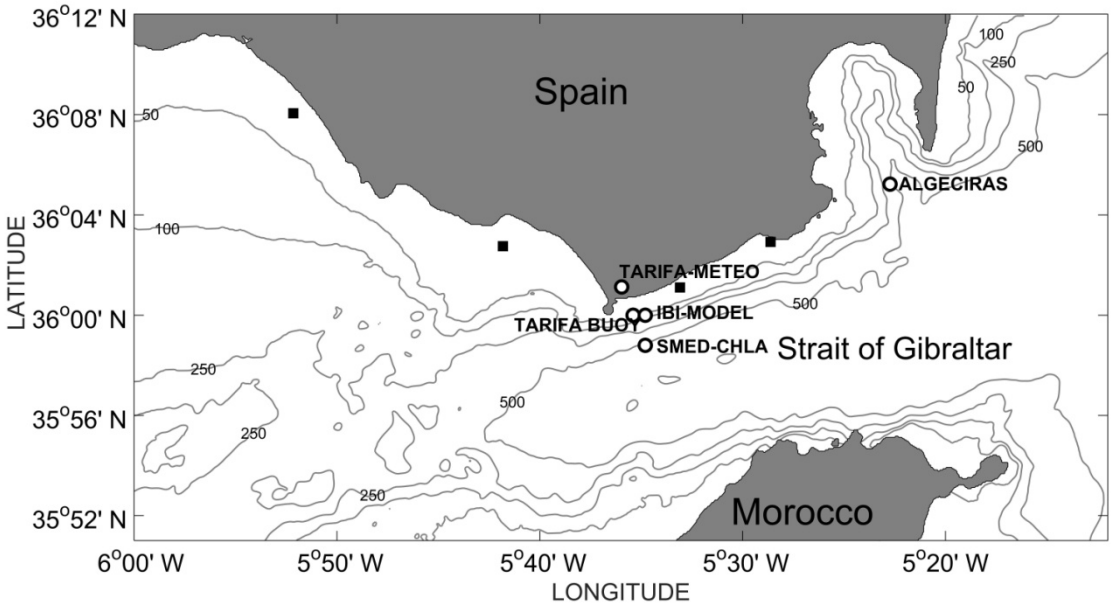

Fig. 2. Time series of air and near surface water temperature. Upper panels show the raw data series. Middle panels represents the trend series. Lower panels indicate the irregular component time series.

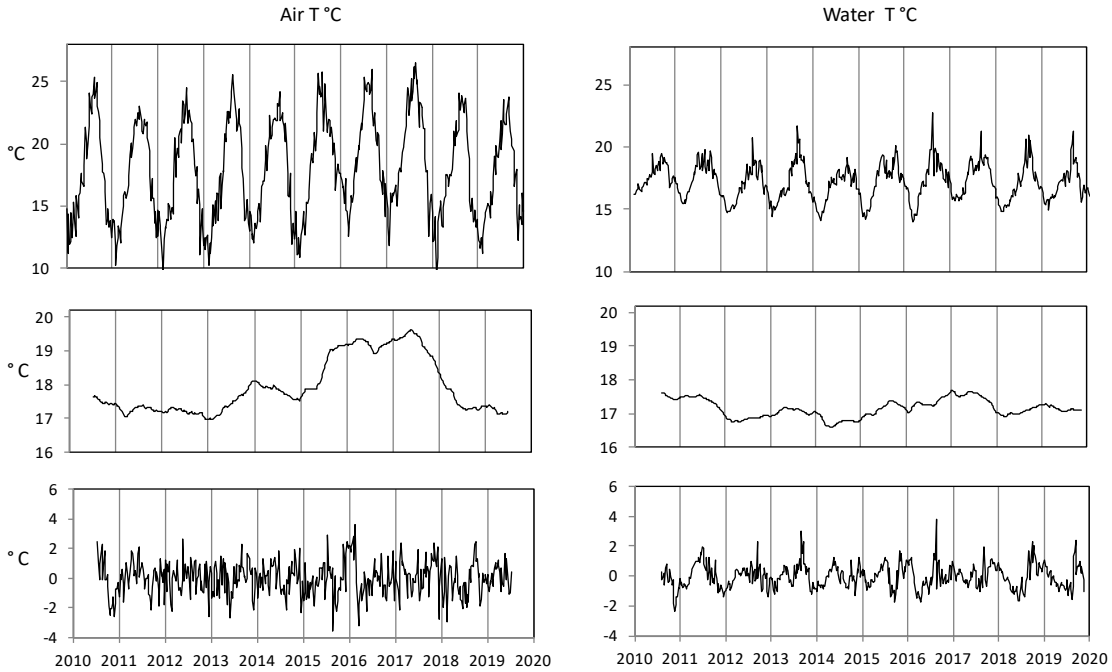

Fig. 3. Time series of salinity and West-East current velocity obtained from the model IBI-MFC (calculated from data from CMENS-Copernicus). Upper panels show the raw time series. Middle panels represent the trends (horizontal dashed line is the mean of the trend series). Lower panels indicate the irregular component time series.

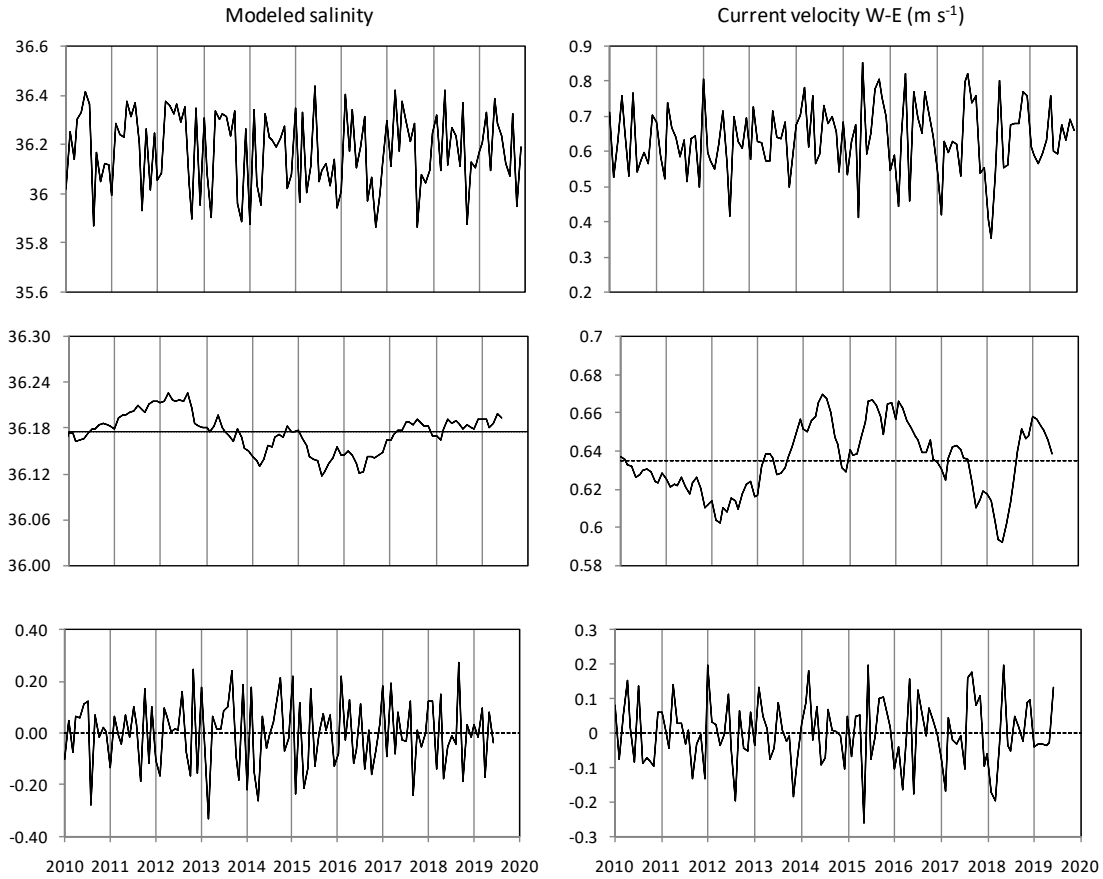

Fig. 4. Time series of nitrate and phosphate concentrations obtained from the model IBI-MFC for the position 36.00ºN, 5.58ºW (CMEMS-Copernicus). Upper panels show the raw data series. Middle panels represent the trend series (horizontal dashed line is the mean of the trend series). Lower panels indicate the irregular component time series.

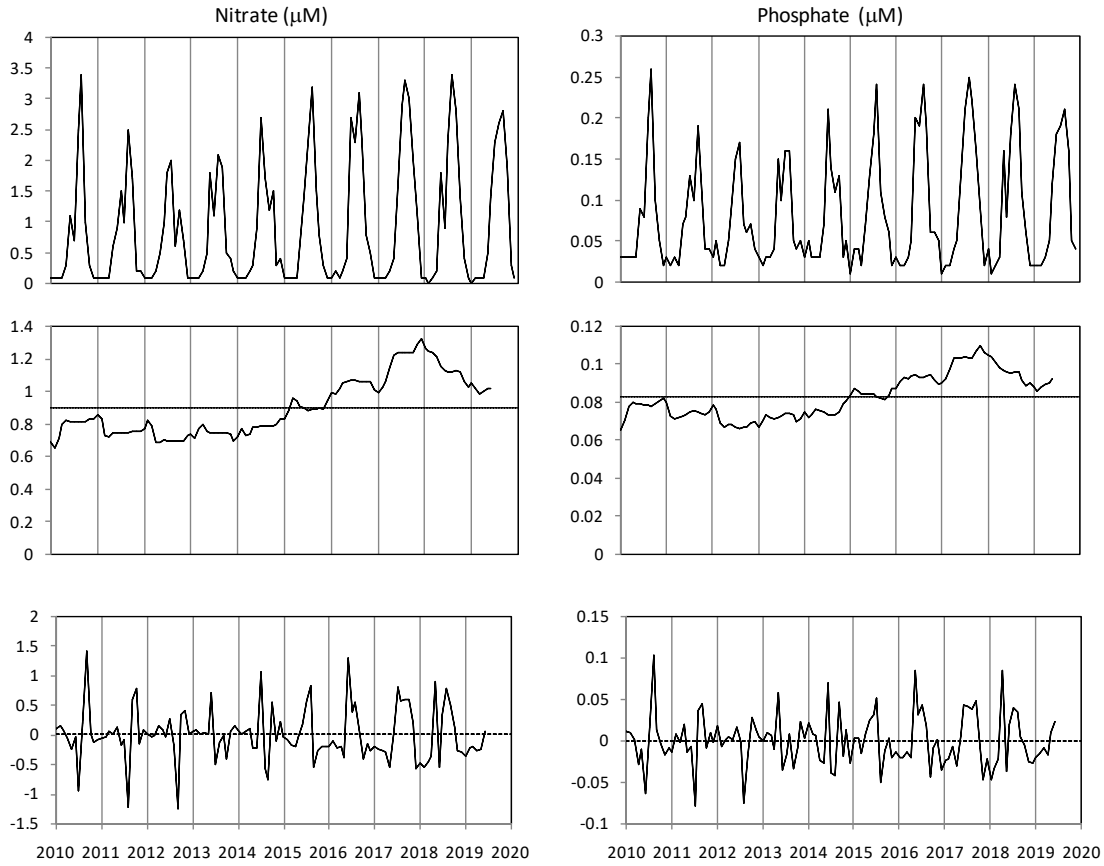

Fig. 5. Results of the PCA performed with the modeled variables with the model IBI-MFC (CMEMS-Copernicus) for the position 36.00ºN, 5.58ºW**. (a)** Biplot of the three first principal components. Variables: Sal, salinity; MLD, mixed layer depth; Nit, nitrate concentration; Phos: phosphate concentration; Chla, chlorophyll *a* concentration; WE, W-E current velocity; T, temperature; Trans, transparency. Time evolution of the three first principal components obtained from the PCA performed with the trend time series of the output variables of the hydro-geochemical model. (b), (c) and (d) represent the time series of scores for the three first PC.

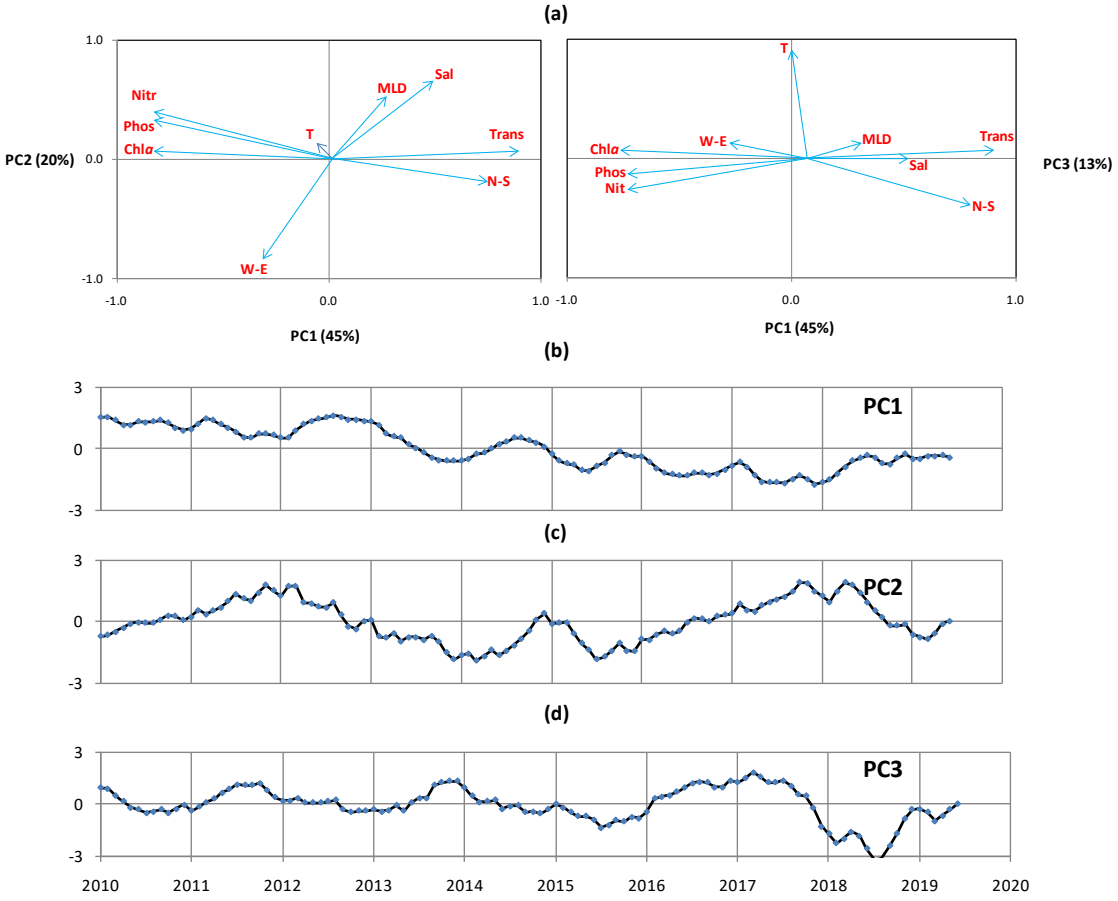

Fig. 6. Annual averaged concentrations of nutrients calculated from data obtained at coastal sampling stations (REDIAM, Junta de Andalucía). The data obtained in the open sea station located close to the Bay of Algeciras are also shown for the surface (0-20 m depth) and deep layer (30-100 m depth). The vertical lines indicate the standard deviation.

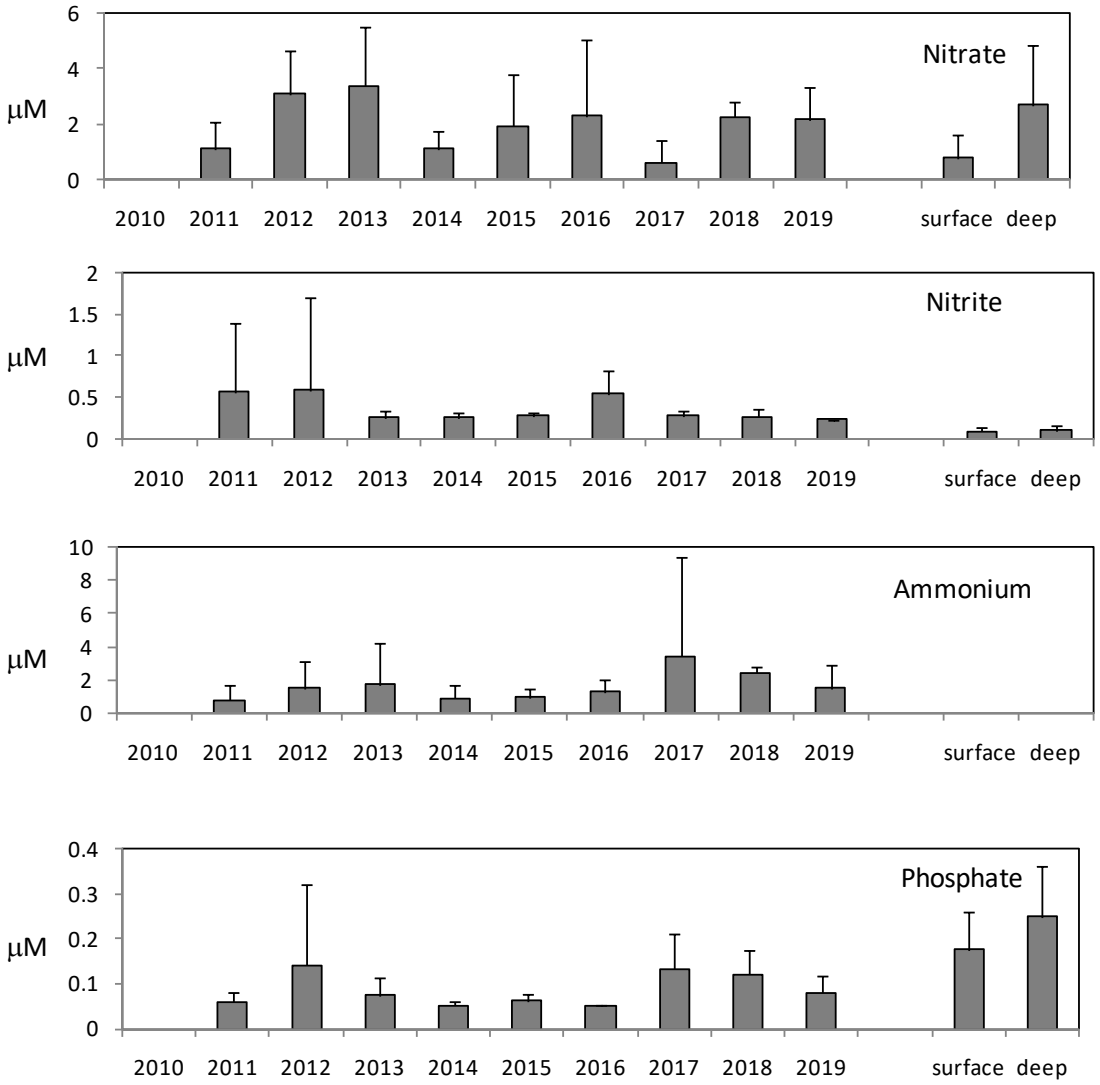

858 **Fig. 7.** Results of the nitrate removal experiments done with *R. okamurae* cultivated
859 under different nutritional conditions. (a) Time course of the nitrate concentration
860 measured in the incubation medium; (b) Nitrate removal rates estimated for the first day
861 of treatment in each incubation vessel (note that each nitrate treatment was assayed by
862 triplicate and that slight differences in the initial concentration were produced at the
863 beginning of the experiments). The continuous line indicates the fitting of the data to the
864 Michaelis-Menten model (r^2 is the coefficient of determination).

865

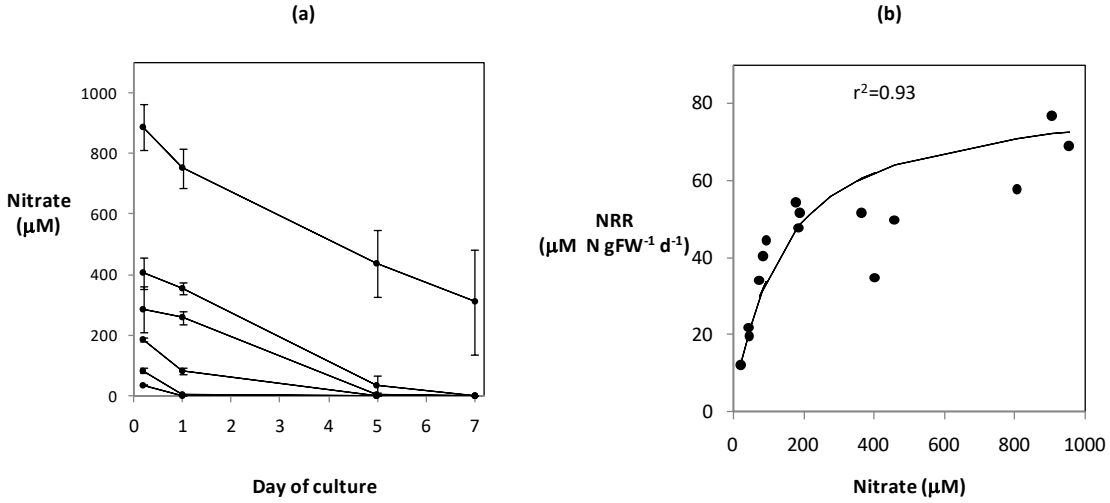

866

867 **Suppl. Fig. 1.** Time series of heatwaves (red lines) and cold spells (blue lines). The
868 maximal intensity (a) and duration (b) of each extreme temperature event are shown.

869

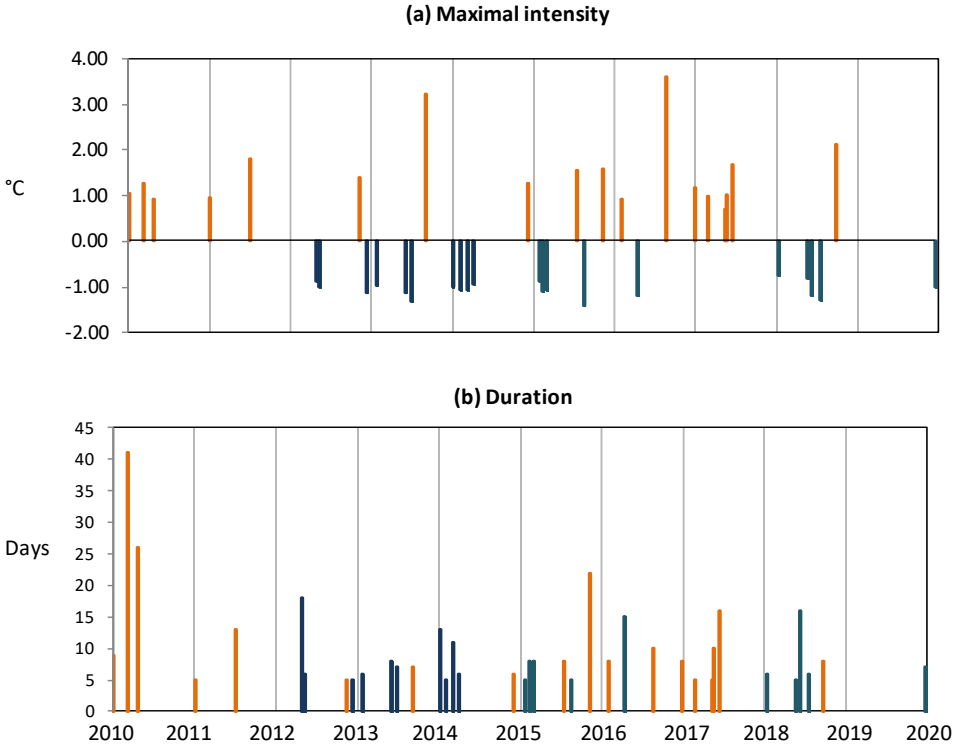

870

871

872

873 **Suppl. Fig. 2.** Time series of satellite chlorophyll *a*. a) raw data series; b) trend series;
874 c) irregular component series.
875
876

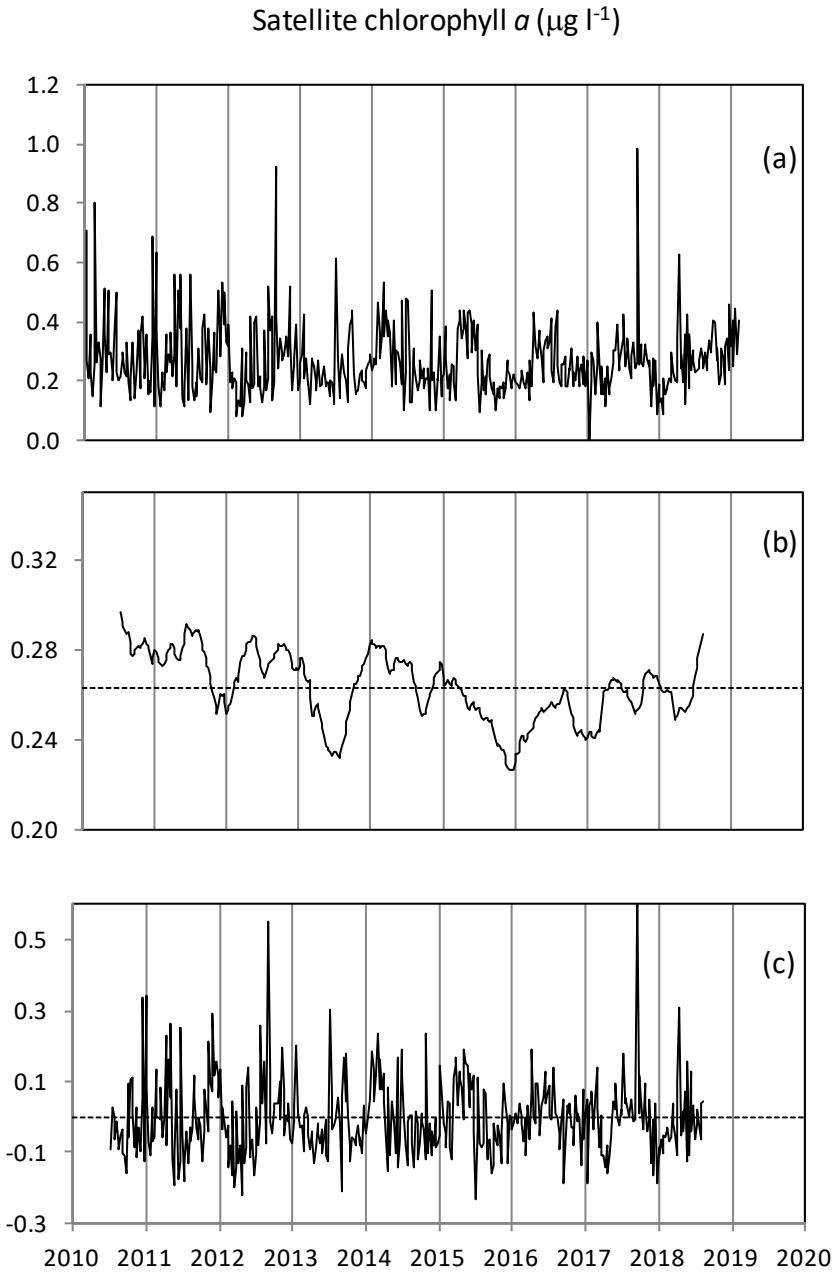

877

878

879

Suppl. Fig.3. (a)Annual mean of salinity calculated from data obtained at coastal and open sea sampling stations. For the open sea station, the data for the surface (0-20 m depth) and deep layer (30-100 m depth) are shown. The vertical lines indicate the standard deviation. (b): relationships between salinity and nitrate concentration for the coastal (opened symbol) and open sea (black symbol) stations. Note that the correlation between salinity and nitrate was not statistically significant for the coastal stations.

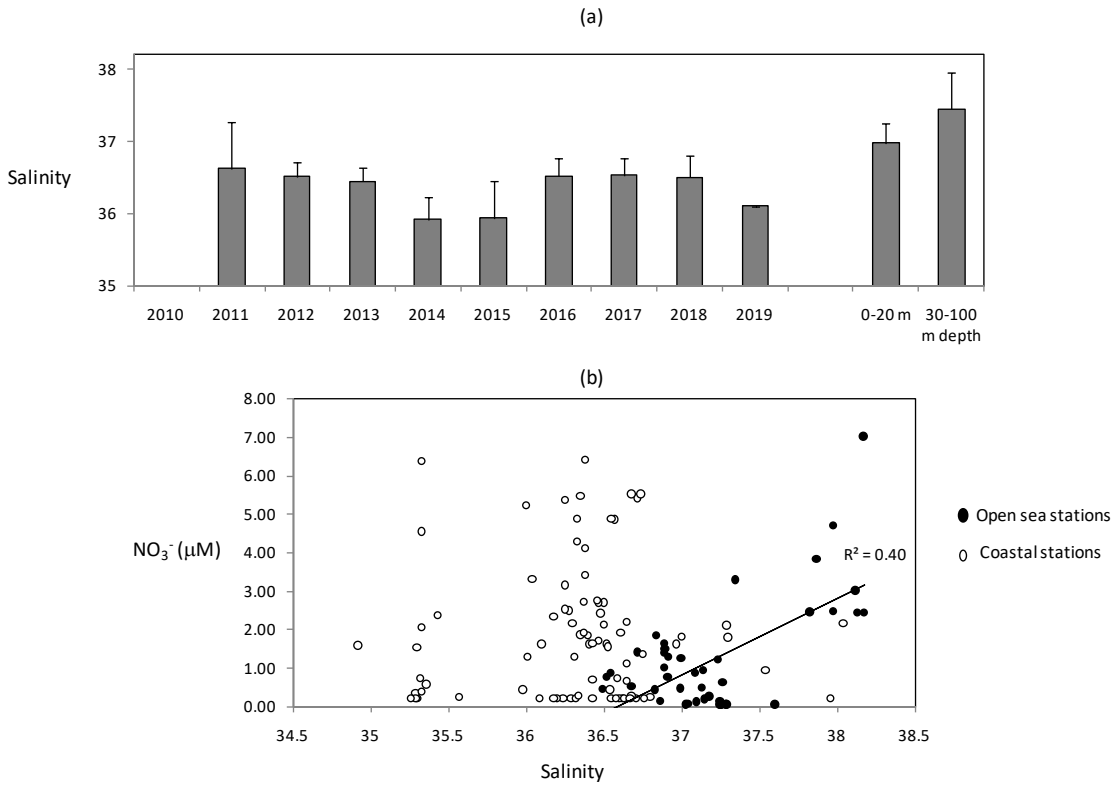

Suppl. Fig. 4. Carbon and nitrogen content averaged for thalli of *Rugulopteryx okamurae* (open square) collected at different times in 2019. Data obtained for other macroalgae collected in 2004 at the southern Iberian Peninsula are shown. The vertical and horizontal lines indicate the variation ranges of C% and N% obtained for the different thalli of *R. okamurae* that have been analyzed. The data for the other algae were fitted to an exponential curve (the determination coefficient is shown).